ANALYSIS OF DIFFERENT SYNCHRONIZATION ALGORITHMS BASED ON PLL, RDFT AND KALMAN FILTER

M. S. Pádua, S. M. Deckmann
School of Electrical and Computer Engineering
State University of Campinas
Campinas, SP, Brazil
marcelo,sigmar@dsce.fee.unicamp.br

F. P. Marafão D. Colón
School of Automation and Control Engineering
Paulista State University
Sorocaba, SP, Brazil
fmarafao,dcolon @sorocaba.unesp.br

Abstract — This paper discusses the main characteristics and presents a comparative analysis of three synchronization algorithms based, respectively, on a Phase-Locked Loop, a Kalman Filter and a Discrete Fourier Transform. Details on how to modify the filtering properties or dynamic response of each algorithm will be discussed in terms of their design parameters. In order to compare the different algorithms, these parameters will be set for maximum filter capability. Then, the dynamic response, during input amplitude and frequency deviations will be observed, as well as during the initialization procedure. So, advantages and disadvantages of all considered algorithms will be discussed.

I. INTRODUCTION

The identification of fundamental amplitude, frequency and phase angle of the power grid voltages has been an important goal related to controlling and synchronizing power electronic devices. In this sense, several algorithms have been proposed and discussed.

The PLL – Phase Locked Loop – has been one of the most applied algorithms to get synchronization signals [1-5]. Recent researches have been shown that RDFT – Recursive Discrete Fourier Transform – can also be applied. Using the information of the RDFT, it is possible to synthesize a unitary synchronizing signal, independently of the input conditions [6-8]. Other possibility is the KF – Kalman Filter, barely, but also applied in some power system applications [9-12]. Each algorithm has its own dynamic and filtering characteristic [13].

The next sections will present the particular details on designing each model, as well as their advantages and disadvantages. In order to perform a comparative analysis, the parameters of all algorithms will be set to achieve maximum filtering characteristics respective to waveform distortions. Afterward, their performance and dynamic response will be analyzed during initialization and voltage or frequency transitory conditions.

II. PLL - PHASE LOCKED LOOP

The analyzed model has been proposed in [1] and is shown in Fig. 1. The voltage signal, v, is directly sampled from the power grid and an orthogonal signal $u_\perp$ is generated by the PLL algorithm when the synchronization is achieved. The average of the inner product (dp) is calculated and compared to a nil reference signal (orthogonality condition). The difference of these two signals is an error signal that is applied to a PI controller. The output of the PI is the fundamental frequency ω of v. This frequency is integrated in order to get the phase function $\theta = \omega t$ of the digitally synthesized orthogonal signal. If a discrete system is used, it is necessary to consider the delay block, where T_s is the sampling period. If the nominal frequency is previously known, it can provide a feed forward signal $\omega_0=2\pi f_1$ in order to improve the initialization dynamic response.

The average of the dot product (dp) can be calculated by means of a moving average filter, which should be tailored as a function of the estimated fundamental frequency (ω). This can be done adjusting either the sampling frequency or the window size according to frequency variations (ω). As discussed in [5], it can be shown that the nonlinear filter transfer function can be simplified by means of Taylor Series, resulting to a linear, constant and unitary gain.

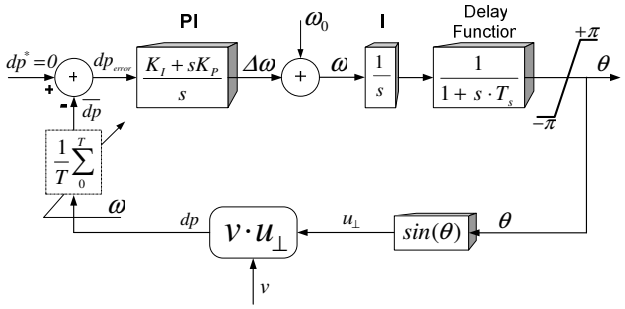

Fig. 1. PLL using inner product of orthogonal functions.

The frequency and the phase angle generated by the PLL are used to synthesize the signal u (1), which is proportional (in-phase) to the fundamental signal of the power grid. If the input voltage is distorted, the PLL algorithm will calculate the fundamental frequency (ω) and phase (θ) of the measured voltage.

$$u = \sin(\theta + 90°) . \quad (1)$$

Since (1) results in a unitary signal, an additional algorithm is needed to calculate the amplitude of the fundamental component. Such algorithm must be sufficiently robust to deal with distorted input voltages. An interesting proposal has been presented in [16] and it is summarized in the Appendix.

Although the normalization of the measured signal is very important to the PLL performance, the gains of the PI controller

are directly related to the dynamic response and effectiveness of the system. Then, the calculations of the PI parameters must be realized very carefully, according to the conditions that the PLL algorithm will be used [1,13]. In this paper, the calculation of such gains is based on the closed-loop transfer function of the linearized model shown in Fig. 2:

$$H_{CL}(s) = \frac{K_P s + K_I}{s^3 T_S + s^2 + K_P s + K_I}. \quad (2)$$

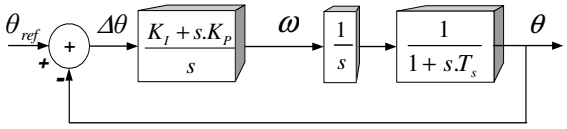

Fig. 2. Simplified model of single-phase PLL.

Null steady-state error for a ramp reference signal is a natural characteristic of a system with structure like the one in (2). But it was not possible to obtain a set of parameters in order to achieve both good filtering and fast response. Thus, the design of the PI should be done considering the most important characteristics, regarding to the final PLL application.

Considering equation (2), while the sampling frequency was sufficiently high, the pole of the transfer function related to it is very distant from the origin and from the other two poles. So such pole can be neglected, yielding a simplified transfer function:

$$H_{CL}(s) = \frac{2\xi\omega_n s + \omega_n^2}{s^2 + 2\xi\omega_n s + \omega_n^2} = \frac{K_P s + K_I}{s^2 + K_P s + K_I}. \quad (3)$$

The gains can be calculated by the second order canonical form:

$$K_P = 2\xi\omega_n, \; K_I = \omega_n^2, \quad (4)$$

where ω_n [rad/s] is the desired closed-loop frequency of the system and ξ is the damping factor, usually between 0.5 and 1.

III. RDFT - Recursive Discrete Fourier Transform

Considering that the RDFT can be calculated in a recursive form [6-8], the model discussed in this paper has been proposed in [13]. A signal v is sampled at a sampling frequency $f_s = 1/T_s = N/T_w$, where T_w is the size of a sliding sampling window and N is the number of samples in the period T_w. Assuming a sequence of samples $k\text{-}N \le n \le k\text{-}1$, $k \ge 1$, the discrete Fourier transform of this sequence, where $v[n] = 0$ if $n \le 0$, is:

$$V_m(k) = V_m(k-1) + (v[k] - v[k-N])\exp\left(-j\frac{2\pi(k-1)m}{N}\right), \quad (5)$$

with $V_m(0) = 0$.

If the nominal fundamental frequency of the power grid is $f_1 = 60$ [Hz], T_w is chosen 1/60 [s]. When T_1 is equal to T_w and $m = 1$, the real part of the inverse transform of (5) results in a filtered signal with the correct amplitude, frequency and phase of the fundamental component. However, in real applications, T_1 can be diferent from T_w. So, the output signal of RDFT results the correct frequency, but the phase and amplitude will be different from the input signal. The RDFT behaves like a band-pass filter tuned on frequency $1/T_w$.

Since it is not possible to change the sampling period in several applications, it will be applied a method of synthesis of an unitary signal $u(k\text{-}N)$, in phase with the measured voltage, which will be useful for adapting the algorithm when $T_1 \neq T_w$.

$$u(k-N) = \cos\left(\varphi(k) + \left(\frac{2\pi(k-1)}{N} + \overline{\Delta\theta}\right)\right), \quad (6)$$

where:

$$\varphi(k) = \tan^{-1}\left(\frac{\mathrm{Im}\{V_1(k)\}}{\mathrm{Re}\{V_1(k)\}}\right), \quad (7)$$

and:

$$\overline{\Delta\theta} = \frac{1}{2}[\varphi(JN+1) - \varphi((J-1)N+1)], \quad (8)$$

where $\varphi(JN+1)$ is the argument (7) of the transform in the beginning of J^{th} interval of T_w, with $J = 1, 2, 3\ldots$ Fig. 3 shows the complet process. In this case, the RDFT will also need an additional amplitude detector, as the one discussed in the Appendix.

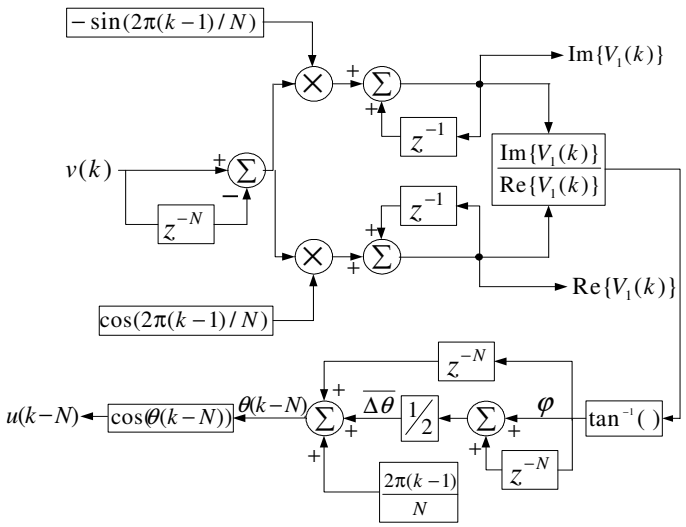

Fig. 3. Blocks diagram of RDFT.

Two methods can be used to fundamental frequency identification. The first one uses the zero-crossing detection of $u(k\text{-}N)$, which is purely sinusoidal. In order to improve the frequency estimation accuracy, an average of the last six values is realized at the end of each cycle of $u(k\text{-}N)$. The second method results from:

$$f_1 \cong \left(\frac{\varphi(JN+1) - \varphi((J-1)N+1) + 2\pi}{2\pi T_w}\right). \quad (9)$$

Both methods are relatively accurate. However, fast transients in the fundamental frequency can be not detected. Nevertheless, since the frequency variations of the power grid

are usually slow, the smooth response of the algorithm is not a disadvantage. Further, the synthesis of $u(k\text{-}N)$ does not depend on the frequency detection and the dynamic response of any control or synchronizing system based on the RDFT will not be affected.

IV. KF – KALMAN FILTER

As discussed in [14,15], consider a system model via state-variables

$$\begin{cases} x_k = Ax_{k-1} + w_{k-1} \\ y_k = Bx_k + z_k \end{cases}, \quad (10)$$

where:

- k is the calculus step,
- $\boldsymbol{x_k}$ is a n x 1 state vector of the system in the step k,
- $\boldsymbol{y_k}$ is a m x 1 vector of the measurement in the step k,
- $\boldsymbol{A}$ is a square matrix n x n, which should be ajusted in case of frequency deviations of the input signals,
- $\boldsymbol{B}$ is a constant m x n matrix,
- $\boldsymbol{w_k}$ is a n x 1 vector representing process noise (due to perturbations and inaccuracy of the dynamic model),
- $\boldsymbol{z_k}$ is a m x 1 vector representing measurement noise (due to the inaccuracy of transducers and signal conditioning circuits) on the signals to be digitalized.

Defining:

- $\boldsymbol{Q}$ – process noise covariance,
- $\boldsymbol{R}$ – measurement noise covariance,
- $\boldsymbol{x_k} - \hat{\boldsymbol{x}}_{k/k-1}$ – initial estimation error,
- $\boldsymbol{P_{k/k-1}}$ – estimation covariance error,
- $\boldsymbol{x_k} - \hat{\boldsymbol{x}}_k$ – final estimation error,
- $\boldsymbol{P_k}$ – final estimation error covariance and
- $\boldsymbol{K_k}$ – Kalman gain,

the state estimation $\hat{\boldsymbol{x}}_k$ based on measurements $\boldsymbol{y_k}$, is achieved in two parts: a prediction step and a correction step, as shown in Fig. 4. The first step estimates the state ahead and gets the error covariance ahead. The second one computes the Kalman gain, update the estimation with measurement and update the error covariance.

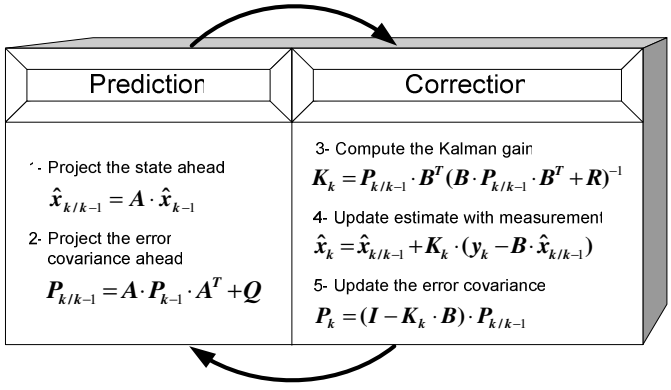

Fig. 4. KF description.

According to [9-12], a good model for the real fundamental wave of a single-phase power system can be represented by means of discrete state-variable model:

$$\begin{cases} \boldsymbol{V_1}(k) = \boldsymbol{A} \cdot \boldsymbol{V_1}(k\text{-}1) + \boldsymbol{w_{k-1}} \\ v(k) = \boldsymbol{B} \cdot \boldsymbol{V_1}(k) + \boldsymbol{z_k} \end{cases}, \quad (11)$$

where $\boldsymbol{V_1}(k) = \begin{bmatrix} v_1(k) \\ v_{1\perp}(k) \end{bmatrix}$ is a vector containing filtered signals in phase ($v_1(k)$) and orthogonal ($v_{1\perp}(k)$) to the measured signal $v(k)$, $\boldsymbol{B} = \begin{bmatrix} 1 & 0 \end{bmatrix}$, $\boldsymbol{w_k}$ has a dimension 2 x 1 and $\boldsymbol{z_k}$, 1 x 1, and

$$\boldsymbol{A} = \begin{bmatrix} \cos(2\pi/N) & -\sin(2\pi/N) \\ \sin(2\pi/N) & \cos(2\pi/N) \end{bmatrix}.$$

Differently from other proposals, as [12], e.g., in this paper the harmonic components are not included in a deterministic way (that is in the very matrix $\boldsymbol{A}$). They will be considered perturbations and in this sense, will be modeled by the measurement and process noises. Considering the harmonics in matrix $\boldsymbol{A}$, even if limiting the maximum order, would be a very complex task.

Thus, the filtered signals in $\boldsymbol{V_1}(k)$ presents the same amplitude of the fundamental component of $v(k)$, what means that the magnitude of the fundamental component is calculated by:

$$M \cong \sqrt{(v_1)^2 + (v_{1\perp})^2}\ . \quad (12)$$

The instantaneous phase angle can be obtained from:

$$\theta(k) = \tan^{-1}\left[-\frac{v_1(k)}{v_{1\perp}(k)}\right], \quad (13)$$

and the fundamental frequency f_1 can be estimated from zero-crossing detection of the signal $\theta(k)$ and improved with an average of the last four estimations.

Matrix $\boldsymbol{A}$ is responsible for the performance of the KF when there is a frequency variation in the input signal. As $N = f_s/f_1$, changing f_1 leads to changing the elements of matrix $\boldsymbol{A}$, if f_s is kept constant. In order to make the KF immune to these disturbs, the identification of f_1 is essential.

The filtering characteristics and the convergence speed of the filter are defined by the measurement noise and process noise. When the measurement noise is high, the trace of $\boldsymbol{R}$ and the elements of $\boldsymbol{K_k}$ will be small. So, the relative weigh of $\boldsymbol{y_k}$ should be reduced in the next calculus of the estimation, what makes the convergence slow. On the other hand, when the measurement noise is small, the trace of $\boldsymbol{R}$ and the elements of $\boldsymbol{K_k}$ will be high, ensuring a better confidence in $\boldsymbol{y_k}$ and a fast dynamic response.

When the process noise is high, the trace of $\boldsymbol{Q}$ and $\boldsymbol{P_{k/k-1}}$ and the elements of $\boldsymbol{K_k}$ are high, resulting in a large reliability for the measurements of $\boldsymbol{y_k}$ in the next estimation step. If the process noise is small, the trace of $\boldsymbol{Q}$ and $\boldsymbol{P_{k/k-1}}$ and the $\boldsymbol{K_k}$ elements are small, resulting in a small weight for $\boldsymbol{y_k}$ and a slow convergence of the algorithm.

Therefore, the KF design depends on conciliation between desired accuracy and dynamic response, what can be achieved by a proper choice of matrices $\boldsymbol{Q}$ and $\boldsymbol{R}$, taking into account input waveform distortions and desired characteristics of final applications [13].

V. SIMULATION RESULTS

In order to compare the discussed algorithms, some simulations has been realized. The sampling frequency was set to $f_s = 12$ kHz. The input signal was defined with unitary amplitude, $f_1 = 60$ Hz, phase angle $\pi/6$ and it is distorted with 10% of 3rd, 5th and 7th harmonics. The parameters of PLL and KF were set to get the maximum filtering capability. The parameters $\omega_n = 22{,}63$ rad/s and $\xi = 0{,}707$ were chosen for the PLL and considering the KF filter,

$$\boldsymbol{Q} = \begin{bmatrix} 10^{-6} & 0 \\ 0 & 10^{-6} \end{bmatrix} \quad \text{and} \quad \boldsymbol{R} = [0.64]. \qquad (18)$$

The THD – total harmonic distortion – of the resulting filtered signals were 0% for the PLL and RDFT and 0.18% for the KF. Fig. 5 shows the estimated fundamental frequency and the errors between the input and output signals for the three algorithms, during initialization. Considering the RDFT, the frequency has been calculated using both methods: zero-crossing detection (right) and by (9) (left). The error signal convergence time has been respectively, 0.3 s, 1.3 s and 2 cycles for PLL, KF and RDFT.

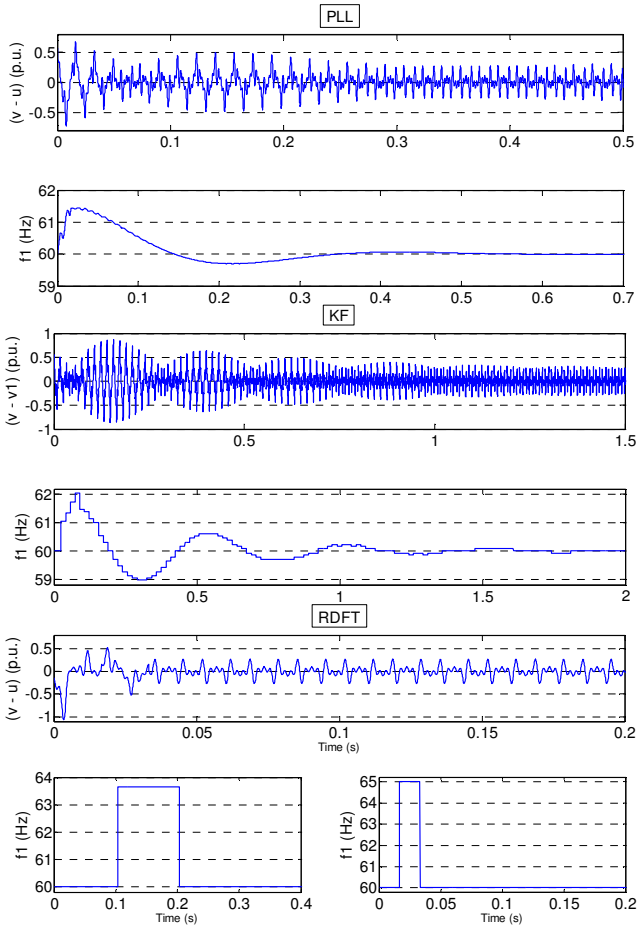

Fig. 5. PLL, KF and RDFT: initialization.

Fig. 6, 7 and 8 show the performance of the methods during a sag about 50% on the input voltage in $t = 2.5$ [s]. The upper graphics show the input and output voltages of the algorithms and the lower part shows the calculated frequency. The output signal converges almost instantaneously in PLL and RDFT and needs 0.5 s to converge in the KF. The frequency does not change in KF. In case of PLL and RFDT, a small perturbation is observed but it is eliminated very rapidly.

Fig. 9, 10 and 11 show the algorithms performance when the fundamental frequency changes to 59 Hz ($t = 2.5$ [s]). The output voltage of RDFT converges almost instantaneously and the PLL and FK output needs 0.3 s and 1 s, respectively. It can be noticed that the resulting frequency signal is somewhat oscillatory for the three algorithms. This could be avoided if the sampling frequency were conveniently altered during the processes. Table 1 summarizes the convergence time and the frequency variation range for all of the algorithms.

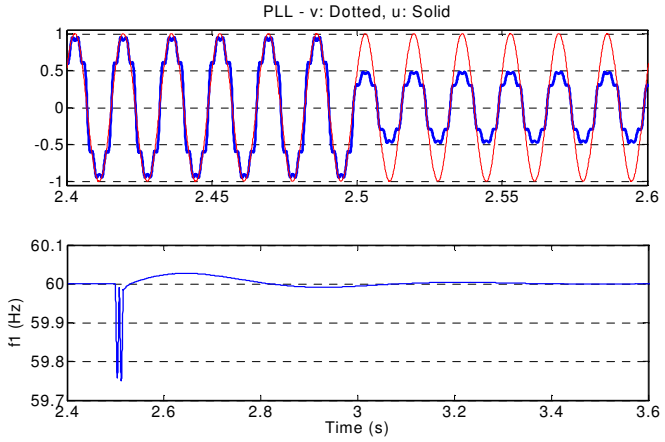

Fig. 6. PLL, voltage sag.

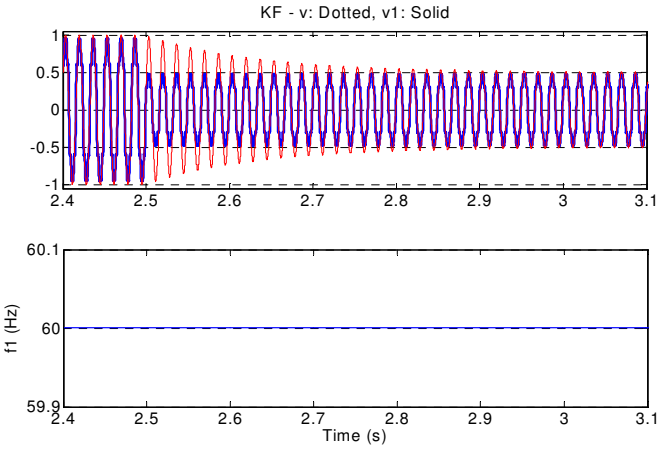

Fig. 7. KF, voltage sag.

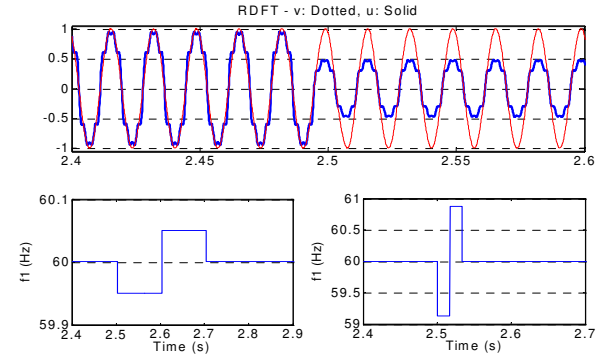

Fig. 8. RDFT, voltage sag.

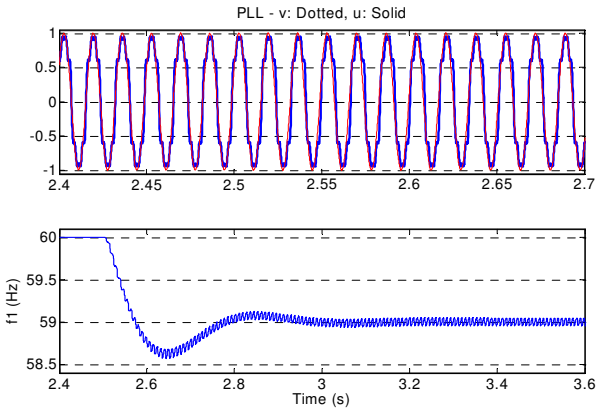

Fig. 9. PLL, fundamental frequency variation.

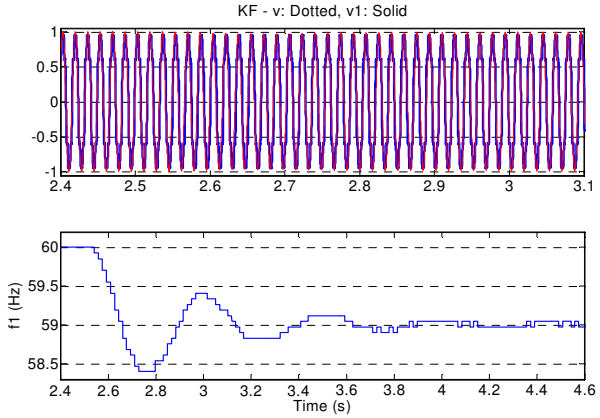

Fig. 10. KF, fundamental frequency variation.

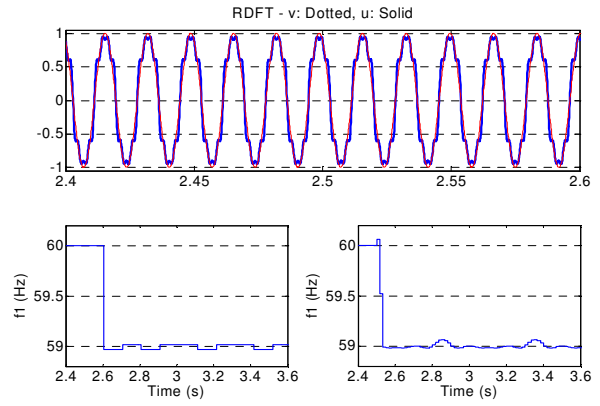

Fig. 11. RDFT, fundamental frequency variation.

Table 1 – Fundamental frequency dynamic.

	Convergence time (s)	**Δf_1 (Hz)**
PLL	0,3	58,95 - 59,05
FK	1,0	58,97 - 59,04
RDFT (Left)	0,1	58,97 - 59,02
RDFT (Right)	0,02	58,98 - 59,07

VI. CONCLUSIONS

This paper has discussed and compared three different algorithms capable of providing synchronism information for grid connected applications. These methods were able to identify the amplitude, frequency and phase angle of the grid voltages. The filtered signals convergence and the calculated fundamental frequency were observed by means of simulation results.

It is important to point out the necessity of choosing among different strategies in order to solve a specific problem, as well as choosing among particular characteristics and desired performance for the algorithms, even when they are contradictory. Such choices are especially important when dealing with the implementation of any system, on which is expected to have good dynamic response under transitory conditions and good accuracy under steady-state.

The PLL algorithm is interesting when a smooth frequency dynamics is required, since f_1 is calculated every sampling step. Moreover, the PLL requires a normalized input signal and an amplitude detector for fundamental identification.

The RDFT results have shown a shorter convergence time and a good filtering capability. However, the dynamic of the frequency estimation is not smooth, because it is updated every cycle. The RDFT algorithm does not require normalized input signals, but it needs an amplitude detector if the frequency is allowed to deviates from the nominal value.

The KF does not require normalization of the measured voltages, or amplitude detectors. However the frequency calculus dynamic is not smooth and, as well as with the PLL, its performance could be smashed if the disturbs in the input signal increases significantly.

Based on the realized studies and previous simulations, it is possible to notice that the RDFT algorithm could be recommended when the filtering capability and convergence time are of major concern; PLL algorithm could be recommended when the frequency estimation is needed every discrete step or when the computational capability is limited (because of its simplicity); the KF importance can be justified since it does not require any complex additional technique to identify the amplitude, frequency or phase angle information. All of them are interesting alternatives to be used in applications with synchronization requirements or fundamental

wave identification. The choice of one or other technique depends basically on the final application requirements.

APPENDIX – FUNDAMENTAL AMPLITUDE DETECTOR

Considering the applications on which the identification of fundamental amplitude may be necessary, the following methodology can be used along with the unitary sinusoids generated, e.g., by the RDFT or PLL presented previously.

Assume that the fundamental and harmonic components of the utility voltage can be expressed by:

$$v = A\sin(\omega t + \varphi) + \sum_{n=2}^{N} C_n \sin[n(\omega t + \varphi)], \qquad \text{(A.1)}$$

where A is the amplitude to be identified, ω is the frequency and φ is the phase of the fundamental component, and Cn is the amplitude of the nth harmonic component.

The digital sinusoid obtained from the PLL or RDFT outputs, which should be in-phase with the fundamental component and has unitary amplitude, can be expressed by:

$$u = \sin(\omega t + \varphi). \qquad \text{(A.2)}$$

Multiplying (A.1) and (A.2) yields:

$$v \cdot u = A\sin^2(\omega t + \varphi) + \sin(\omega t + \varphi)\sum_{n=2}^{N} C_n \sin[n(\omega t + \varphi)] \qquad \text{(A.3)}$$

Since all product terms containing different frequency components have zero mean value, the resulting mean value of (A.3) reduces to the mean of the first squared term:

$$\overline{v \cdot u} = \frac{A}{2}, \qquad \text{(A.4)}$$

Hence, the amplitude of the fundamental component of the utility voltage is given directly by:

$$A = 2 \cdot \overline{v \cdot u}. \qquad \text{(A.5)}$$

Fig. 12 illustrates the fundamental amplitude detector. Since the PLL or the RDFT can be used, the proposed scheme is immune to voltage distortions or frequency deviations and it is not based on any sort of voltage peak detector.

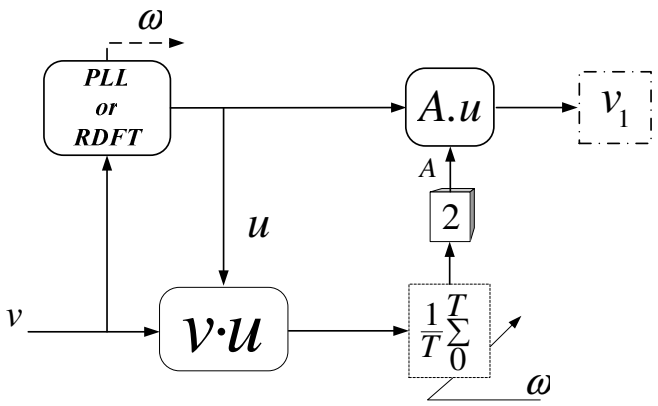

Fig. 12 – Fundamental Amplitude Detector.

REFERENCES

[1] F. P. Marafão, S. M. Deckmann, J. A. Pomilio, R. Q. Machado, "Metodologia de Projeto e Análise de Algoritmos de Sincronismo PLL", *Eletrônica de Potência*, vol. 10, no. 1, June 2005 (in portuguese).

[2] V. Kaura and V. Blasko, "Operation of a Phase Locked Loop System under Distorted Utility Conditions", IEEE *Transaction on Industry Applications*, vol. 33, no. 1, pp. 58-63, 1997.

[3] L. G. B. Rolim, D. R. Costa Jr. and M. Aredes, "Analysis and Software Implementation of a Robust Synchronizing PLL Circuit Based on the pq Theory", *IEEE Transaction on Industrial Electronics*, vol. 53, no. 6, pp. 1919-1926, 2006.

[4] H. Awad, J. Svensson, and M. J. Bollen, "Tuning Software Phase-Locked Loop for Series-Connected Converters", *IEEE Transactions on Power Delivery*, vol. 20, Nº. 1, pp. 300-308, 2005.

[5] F.P. Marafão, S.M. Deckmann and E.K. Luna, "A Novel Frequency and Positive Sequence Detector for Utility Applications and Power Quality Analysis", *International Conference on Renewable Energy and Power Quality* (ICREPQ), Spain, 2004.

[6] B. P. McGrath, D. G. Holmes and J. Galloway, "Power Converter Line Synchronization Using a Discrete Fourier Transform (DFT) Based on a Variable Sample Rate", *IEEE Transactions on Power Electronics*, vol. 20, no. 4, pp. 877-844, 2005.

[7] S. Srianthumrong, and S. Sangwongwanich, S, "An Active Power Filter with Harmonic Detection Method based on Recursive DFT. *8th International Conference on Harmonics And Quality of Power*, vol. 1, pp. 127-132, Greece, 1998.

[8] J. A. R. Macías and A. G. Expósito, "Efficient Moving-Window DFT Algorithms". *IEEE Transactions on Circuits and Systems II: Analog and Digital Signal Processing*, vol. 45. no. 2, pp. 256-260, 1998.

[9] S. Liu, "An adaptive Kalman filter for dynamic estimation of harmonic signals", *8th International Conference on Harmonics and Quality of Power*, vol. 2, pp. 636-640, Greece, 1998.

[10] M. V. Ribeiro, S. M. Deckmann, and J. M. T. Romano, "Adaptive filtering, wavelet and lapped transforms for power quality problem detection and identification", *International Symposium on Industrial Electronics (ISIE '03)*, vol. 1, pp. 301-306, Brazil, 2003.

[11] W. Rebizant, D. Bak, and J. Szafran, "High-speed measurements with adaptive Kalman filter", *8th IEE International Conference on Developments in Power System Protection*, vol. 1, pp. 52-55, 2004.

[12] R. Cardoso, and H. A. Gründling, "Single and Three-Phase Kalman Filter Based Synchronization Methods", *IEEE 7th International Conference on Industrial Applications (INDUSCON)*, Brazil, 2006.

[13] M. S. Pádua, Técnicas Digitais para Sincronização com a Rede Elétrica, com aplicação em Geração Distribuída, Dissertação de Mestrado, UNICAMP, Campinas, 2006 (in portuguese).

[14] R. E. Kalman, "A new approach to linear filtering and prediction problems", *Transaction of the ASME - Journal of Basic Engineering*, pp. 35-45, 1960.

[15] H. W. Sorenson, *Kalman Filtering: Theory and Application*, IEEE Press, New York, 1985.

[16] M. S. Pádua, S. M. Deckmann, and F. P. Marafão, "Frequency-Adjustable Positive Sequence Detector for Power Conditioning Applications", *IEEE 36th Annual Power Electronics Specialists Conference (PESC)*, pp. 1928-1934, Brazil, 2005.